ASTRONOMY & ASTROPHYSICS
SUPPLEMENT SERIES

Astron. Astrophys. Suppl. Ser. **117**, 369-375 (1996)

Penetrating the "zone of avoidance".* III. A survey for obscured galaxies in the region $120^\circ \le \ell \le 130^\circ, -10^\circ \le b \le +10^\circ$

G. Lercher, F. Kerber and R. Weinberger

Institut für Astronomie der Leopold-Franzens-Universität Innsbruck, Technikerstraße 25, A–6020 Innsbruck, Austria
http://ast7.uibk.ac.at

Received September 18; accepted November 21, 1995

Abstract. — As the third part in a series of papers on galaxies in the "zone of avoidance" (ZOA) of the Milky Way we present a compilation of 1161 galaxies discovered during a systematic search on Palomar Observatory Sky Survey (POSS) red-sensitive prints. The region searched comprises 200 square degrees, at $120^\circ \le \ell \le 130^\circ, -10^\circ \le b \le +10^\circ$. In addition to galactic, equatorial and rectangular coordinates, we list maximum and minimum optical diameters derived from both the red- and blue-sensitive prints, could assign a morphological type to some of the objects and made cross-checks with the IRAS PSC and several radio catalogues. A test for completeness suggests, that our catalogue should be complete down to a limiting galaxy-diameter of $0\farcm35$. An asymmetric distribution of the galaxies with respect to the galactic equator was found and is discussed by comparing it with the locations of optically visible dust clouds and/or the distribution of IR-emitting dust material. A comparison between the distribution of the galaxies and the $100\,\mu$ IRAS intensity maps led to the identification of four possible clusterings. As a byproduct of our galaxy search, two new planetary nebulae, nebulous stars at the position of a strong cold IRAS point source, and a nearby dwarf irregular galaxy could be detected.

Key words: catalogs — (ISM): dust, extinction — Galaxy: structure — galaxies: general — galaxies: clusters of

1. Introduction

Extragalactic research in the "zone of avoidance" (ZOA) of our Galaxy is, for about half a decade, a quite booming area. A flourishing identification industry has led to the discovery of many thousand mainly optically identified extragalactic objects in a zone that was, by Hubble (1934), found to be practically devoid of galaxies. This (still speeding up) development was and is, from a purely scientific point of view, triggered by several developments. One is the discovery of large-scale structures in the Universe and the insight that these structures will, of course, not come to a halt when approaching the ZOA. A second are the discussions about the Great Attractor that was suspected to be located at low galactic latitudes. From a technical point of view, the development of highly sensitive instrumentation, like CCD's and IR arrays, and the progress in radial velocity measurements in, e.g. H I, all forcefully promoted the research in this field. Very recently, scientists also take the pick out of the bunch by the discovery and investigation of highly obscured, nearby galaxies (Kraan-Korteweg et al. 1994; Huchtmeier et al. 1995).

Due to the favourable plate material (fine grain emulsions and considerable deepness), optical surveys for galaxies were particularly promising for the southern hemisphere. Major surveys there are those performed by Kraan-Korteweg (1989) and Kraan-Korteweg & Woudt (1994), Saito et al. (1990, 1991), and Yamada et al. (1993).

In the northern hemisphere, due to the fact that only a small fraction of the new deep POSS II atlas is available by now, the POSS I-E (red-sensitive) prints with a stellar limiting magnitude of $20\fm0$ are still the best choice for an analogous search: The first large-scale survey was carried out by Weinberger (1980) who examined a 4° wide strip along the entire northern galactic plane. A considerably extended search in the north on the same material, up to at least $|b| \le 5^\circ$, but in a few areas up to $|b| \le 10^\circ$ was started by a group of astronomers at Innsbruck six years ago and could be finished quite recently. For preliminary overviews of the Innsbruck project and of the region investigated in this article see Seeberger et al. (1994) and Lercher (1994), respectively. First detailed results can be found in the first (hereafter Paper I) and second of our

---

Send offprint requests to: G. Lercher

*Table 2 is only available in electronic form at the CDS via anonymous ftp 130.79.128.5

series of papers (Weinberger et al. 1995, and Seeberger et al. 1995). In the present study (representing the main part of the master thesis of the author G. Lercher) we describe and discuss the results of a survey for optically visible galaxies in a particular region in the northern galactic plane.

2. Motivation and method

The main reasons for selecting the area from $\ell = 120°$ to $130°$ and from $b = -10°$ to $+10°$ were as follows:

1. The region is in the second galactic quadrant, where a statistically relevant but not too large galaxy sample can be expected.
2. The famous Maffei galaxies (Maffei 1 and 2) are located only a few degrees away; therefore, other nearby object(s) might be detectable (this assumption has meanwhile be proven by the discovery of two nearby galaxies: a massive one - see Kraan-Korteweg et al. (1994), and this massive object plus a dwarf irregular - see our last section and Huchtmeier et al. (1995). In addition McCall & Buta (1995) reported the detection of another two dwarf companions of Maffei 1).
3. The region is free of large extended emission nebulae or dust clouds.

The examination of the POSS I prints was carried out by aid of a binocular microscope with a 16-fold magnification. The POSS I fields fully or partially searched are listed in Table 1.

Table 1. The fields of the POSS I searched for our program

field no.	center(1950.0)	field no.	center(1950.0)
945	$+54°$ 1^h16^m	1237	$+54°$ 0^h38^m
1240	$+60°$ 1^h28^m	596	$+60°$ 0^h44^m
878	$+66°$ 1^h44^m	1234	$+66°$ 0^h52^m
555	$+66°$ 0^h00^m	1230	$+72°$ 2^h16^m
1218	$+72°$ 1^h08^m	1217	$+72°$ 0^h00^m

We checked all the objects by taking into account also the blue-sensitive (O) prints and by including, close to the galactic plane, the prints of the Infrared Milky Way Atlas (Hoessel et al. 1979). A lower limit for the diameter of galaxies of about $0\rlap{.}'1$ was chosen. The latter atlas was of great value in many cases, since the discrimination against H II regions and most reflection nebulae was thus considerably eased.

3. Results and discussion

3.1. *The catalogue*

In Table 2 we list our 1161 galaxy candidates in order of increasing galactic longitude. The galaxy designations follow the IAU recommendation for the nomenclature of new objects: ZOAG G$\ell\ell\ell.\ell\ell \pm bb.bb$ (see Paper I). ZOAG means "Zone of Avoidance Galaxy", G stands for galactic coordinates, and $\ell\ell\ell.\ell\ell$ and $\pm bb.bb$ are galactic longitude and latitude, respectively.

In Col. 1 the designation of the galaxies is given. For reasons of brevity the prefix ZOAG G is omitted. In a few cases, a suffix "a" or "b" is added. Its meaning is described in Paper I. A colon means, that a galactic nature of the object couldn't be excluded. Columns 2 and 3 give the equatorial coordinates for epoch 1950.0, Cols. 4 and 5 for epoch 2000.0. Columns 6 to 8 refer to identifications on the POSS I: in Col. 6 the POSS I field number is listed; Cols. 7 and 8 give rectangular coordinates (in mm) of the galaxies with the origin at the south-east corner of the fields. Both rectangular and equatorial coordinates were determined using a high-resolution digitizer and a suitable software developed at Innsbruck. A set of 7 to 11 standard stars from the SAO-catalogue was used to compute these coordinates. The overall accuracy is $\pm 6''$. In Cols. 9 and 11 we present maximum and minimum diameters (in arcmin) measured from POSS I red-sensitive (E) and blue-sensitive (O) prints, respectively. When no value is given, there is no galaxy visible on the O-print. In a number of cases a core surrounded by diffuse emission can be seen: then, the maximum and minimum core diameters (in arcmin) measured on POSS I-E and O prints are listed in Cols. 10 and 12. No value means that no core is traceable.

One might wonder why no galaxies with a diameter of $0\rlap{.}'25$ are listed. This is an artificial effect which occurs when converting measured diameters from mm to arcmin and rounding to $0\rlap{.}'05$. The error of the given diameters induced by this procedure is not more than $0\rlap{.}'025$, much smaller then the expected accuracy of about $0\rlap{.}'05$ to $0\rlap{.}'1$ of the measurements itself.

A morphological classification of reddened galaxies is rather uncertain. For example, a heavily obscured spiral galaxy would nothing retain but its bulge and could thus be misclassified as an elliptical (Cameron 1990). We classified (in Col. 13; t = type) spirals as S and probable spirals as S?. In Col. 14 galaxy names, IRAS-PSC designations and radio source designations are given. For $|b| \leq 5°$ galaxy names are taken from Paper I, for $5° < |b| \leq 10°$ names are taken from the POSS I overlays. For cross-identifications with the IRAS catalogue we used our above-given positional uncertainty and checked whether our optical error bars fell within the IRAS uncertainty ellipse or not. Cases with two galaxies located inside one IRAS error ellipse are marked by asterisks.

3.1.1. Completeness of the catalogue

Plotting the number of galaxies having diameters larger or equal to a given limit versus this very limit enables one to estimate the completeness of the catalogue in a rough way. Assuming a mean linear galaxy diameter and a homogeneous distribution in space, one expects a linear relationship with a slope of -3 between the logarithms of both the number and diameter limit of the galaxies. Figure 1 suggests that our catalogue should be complete down to 0.′35. One has, however, to be aware that for lower galactic latitudes, due to the poorer statistics in these regions, the value of 0.′35 is no more valid.

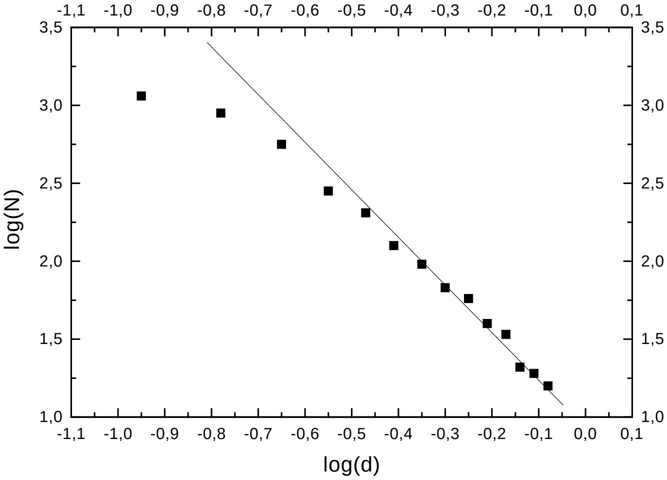

Fig. 1. Squares: logarithm of the total number of galaxies down to a given angular diameter versus the logarithm of this very diameter. The line corresponds to the expected slope of −3

3.2. *Distribution of galaxies*

In Fig. 2b the distribution of the 1161 galaxy candidates is shown.

The number of galaxies at negative galactic latitudes is much larger than at positive ones. The nominal galactic equator does not coincide with the dust layer, since there appears to be much more dust above the galactic plane than below.

The distribution of galaxies can be influenced by two ways, i.e. it can be of i) galactic (i.e. foreground) origin and/or it can ii) reflect the true distribution, like concentrations (clusters) of galaxies. The former possibility might, in part, be tested by comparing the galaxy distribution with existing maps of dust clouds or emission nebulae. In Fig. 2a the distribution of dark clouds in the region of interest, taken from Lynds (1968), is shown: prominent (i.e. close) dark clouds cover only a small fraction of the region, but might be responsible for the prominent lack of galaxies in/near the galactic plane in the western part of Fig. 2b. Bright emission nebulae might also cover and hide galaxies on the POSS, but are very few in number and are negligible as to their effect.

3.3. *The* $100\,\mu$ *sky brightness and projected density of galaxies*

The IRAS Sky Survey Atlas (Wheelock et al. 1993) provides sky brightness images in the 12, 25, 60 and $100\,\mu$ IRAS-bands. The 60 and $100\,\mu$ images can be used as a means for discussing the distribution of the IR emitting dust (see e.g. Wakamatsu et al. 1994). Figure 2c shows the sky surface brightness of the surveyed region at $100\,\mu$. Emission due to zodiacal light is already subtracted. To test whether a correlation exists between the $100\,\mu$ sky brightness and the measured galaxy surface density, we subdivided the whole dynamical range of the $100\,\mu$ image into 100 equidistant intensity bins of 2 m Jy/sr each. Then we calculated the number of our galaxy candidates that are located within the i-th bin ($N^i_{\rm G}$). Dividing this number by the number of pixels within the i-th intensity bin ($N^i_{\rm P}$), gives the number of galaxies per pixel and intensity bin (ρ^i). The 2 m Jy/sr range of the bins was chosen to ensure that on the one hand structures within the $100\,\mu$ image are resolved as good as possible and on the other hand enough galaxies are found within each bin to provide good statistics.

Squares in Fig. 3 show the resulting ρ^i versus their corresponding $100\,\mu$ intensities. The errorbars represent $\sqrt{N^i_{\rm G}}/N^i_{\rm P}$. One notices a clear correlation between galaxy density and $100\,\mu$ intensity. We interpret this result that $100\,\mu$ IRAS sky brightness maps trace the two-dimensional dust distribution in the galactic plane sufficiently well. The small peak visible at the 34−36 mJy/sr bin does not seem to be caused by a real overdensity, as the two-dimensional distribution of the galaxies located within this bin shows a homogeneous distribution. Figure 3 shows no further peak or flattening. This means, that within the surveyed region we deal with either a homogeneously distributed galaxy population, or possibly existing overdensities are smoothed out by the overall galaxy distribution located within the i-th $100\,\mu$ intensity bin.

Figure 2b reveals four overdensities centered at $(\ell, b) = (128.0, 8.9)$ (Candidate I), (124.5, 8.6) (II), (129.9, 3.6) (III) and (120.5, −9.5) (IV). Taking into account Fig. 3, an analysis of these four clustering candidates can be performed comparing Fig. 2b and Fig. 2c.

Candidate I: It is located within a faint emission hole in the $100\,\mu$ map. However its galaxy density is higher than the density within the extended emission hole centered at about $(\ell, b) = (124.5, 9.0)$, which has intensities around 10−11 mJy/sr. This is about 4 to 5 mJy/sr below the lowest $100\,\mu$ intensities in the region of Candidate I. Therefore, according to Fig. 3, the area around $(\ell, b) = (124.5, 9.0)$ should have about twice the galaxy density of the region of Candidate I. Figure 2b shows, that the opposite situation is the case. In addition the intensity in the densest part of Candidate I is about 2 m Jy/sr higher then in the minimum of the faint emission hole. Thus we are led to the suggestion that Candidate I is indeed a real overdensity.

Candidate II: It is located at the edge of the emission hole centered at $(\ell, b) = (124.5, 9.0)$. Although obvious to the

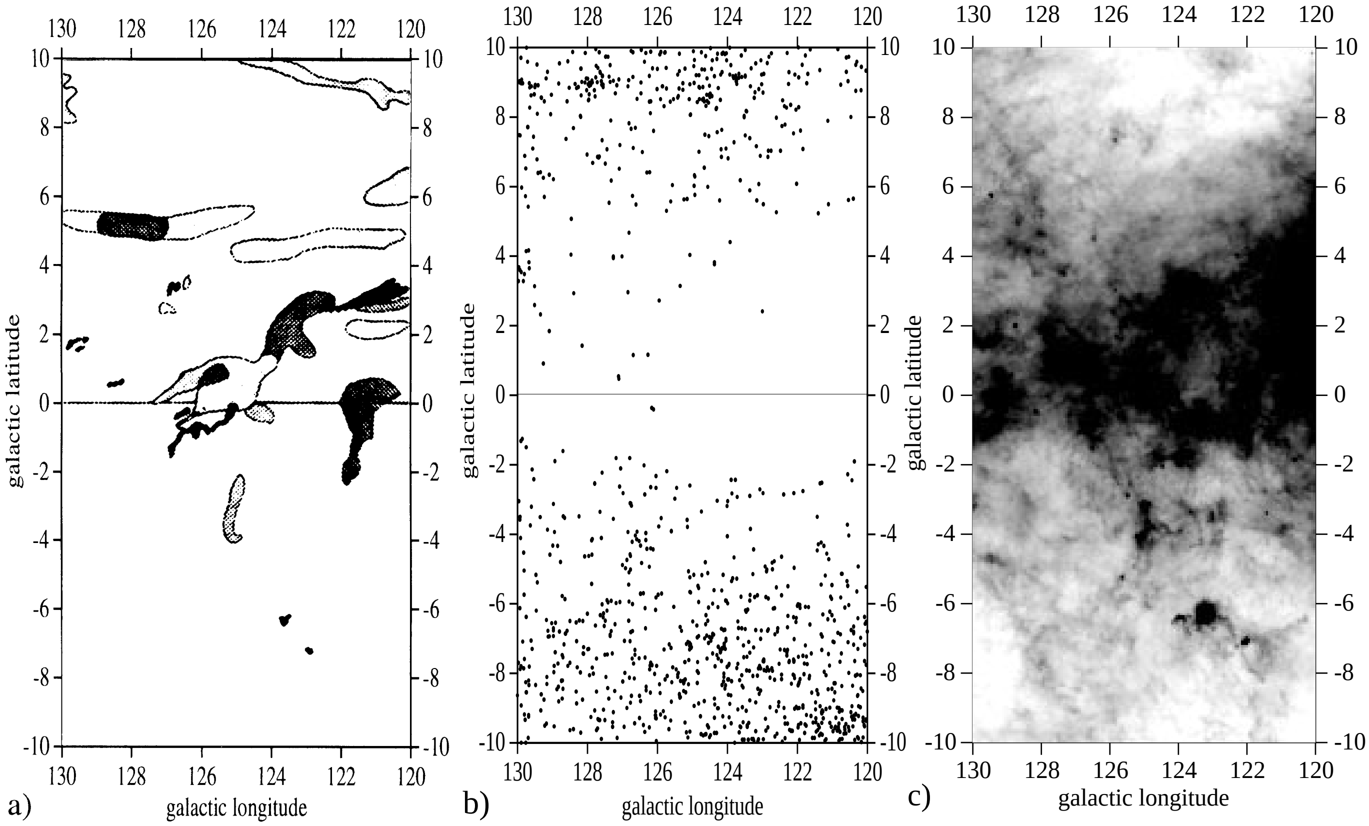

Fig. 2. The distribution of dark clouds from Lynds (1968) **a)**, of our galaxy candidates **b)**, and the sky surface brightness at $100\,\mu$ **c)**. Pixels in **c)** correspond to $4' \times 4'$ cells. Pixels with lowest $100\,\mu$ intensities are white, those with highest ones black

eye, the significance of this clustering remains uncertain when the foreground $100\,\mu$ intensity is taken into account.

Candidate III: It is located within an $100\,\mu$ emission hole centered at about $(\ell, b) = (130.0, 3.5)$. However there is an equally "deep" and extended hole at about $(\ell, b) = (128.5, 3.1)$ within which only two galaxies have been found (10 for Candidate III). This is not explicable with a homogeneous galaxy distribution. In addition according to Fig. 3 at these intensities (25−26 mJy/sr for Candidate III) we expect heavy extinction and therefore much smaller galaxy densities.

Candidate IV: Comparing the observed galaxy density with the expected density (see Fig. 3) suggests that this is a significant overdensity. Due to the fact that Candidate IV is located close to the edge of the survey field, further studies are needed to confirm this suggestion.

Radial velocity measurements will be able to clarify the nature of all four candidates.

One remark concerning quality differences in the survey material should be made: The limiting magnitude of different POSS-I prints may differ by as much as 0.5^{m}. This means that quality differences between single prints may cause print-dependent galaxy counts. The galaxies visible on overlapping regions of the POSS fields 945 and 1237 show this effect. E-diameters from 945 are on average $0'.05$ smaller. We therefore think that at least part of the jump in galaxy counts visible at $\ell = 125°$ and $-10° < b < -5°$ is due to such a quality difference.

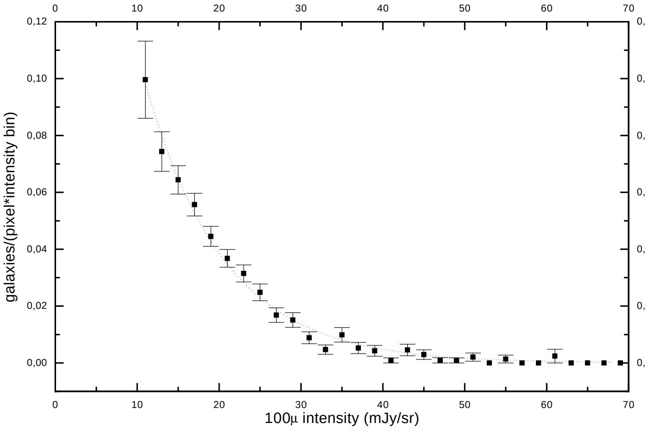

Fig. 3. Squares: the number of galaxies per pixel and intensity bin of Fig. 2c ρ^i, plotted versus the corresponding $100\,\mu$ intensity

Consequently, Fig. 3 represents the mean of 10 (see Table 1) somewhat different 100 μ intensity ↔ galaxy density correlations.

4. Byproducts of our search

During the search for galaxies on the red-sensitive POSS I-E prints we found several hitherto unknown nebular objects, the most interesting ones being two planetary nebulae, a tiny grouping of very faint nebulous stars, and a roundish source that originally defied a quick determination of its nature but eventually turned out to be a nearby dwarf irregular galaxy. The two planetary nebulae (PNe), at (1950) $\alpha = 00^{\rm h}59^{\rm m}12\overset{\rm s}{.}3, \delta = +65^\circ30'29''$ and at $\alpha = 01^{\rm h}36^{\rm m}50\overset{\rm s}{.}0, \delta = +56^\circ19'33''$, are included in a compilation of new PNe by us (Kerber et al. 1994), will be observed together with these and are consequently not further described here. The remaining two objects, however, deserve to be discussed in the following.

4.1. *IRAS 00412+6638, a cold galactic point source*

On POSS I-E and O 1234, on the Infrared Milky Way Atlas (Hoessel et al. 1979) and especially on the POSS II-R film copy No. 79 a tiny grouping of very faint nebulous stars is visible. At the position of the grouping there is a strong “cold” IRAS point source. Sources of this kind received a lot of attention in recent years, since they might represent early stages in the formation of low-mass stars. The object in question was included in several surveys (Casoli et al. 1986; Wilking et al. 1989; Wouterloot & Brand 1989). The latter authors report non-Gaussian CO emission profiles and assign them to a distant (−68.1 km/s; 7.11 kpc) and a nearby source (−4.65 km/s; 0.42 kpc).

Interestingly, IRAS 00412+6638 is known throughout as an “optically non-detected” source. Casoli et al. (1986) unsuccessfully searched for optical identifications. Optical identifications of cold IRAS point sources, particularly as to the presence of nebulae, are rare and consequently of considerable interest: out of the 96 objects contained in Table 2 of Casoli et al. (1986), only five are reported to show nebulosity.

We obtained a CCD $R_{\rm c}$-band frame at the 1.8 m telescope of the Asiago Observatory (Fig. 4). There are two subgroups visible, both immersed in nebulae or nebular-like emission: the upper (northern) one consists of at least half a dozen stars (the brightest star at top of the group is a foreground object), the southern group of at least 4 to 5 stars. Due to the nebulous appearance of about equal amount on all the sky survey prints and films noted above we think that we deal with reflection nebulae. The division into two subgroups might be real or caused by dust obscuration, but cannot be decided on the basis of our material. Anyway, we obviously deal with a star forming region.

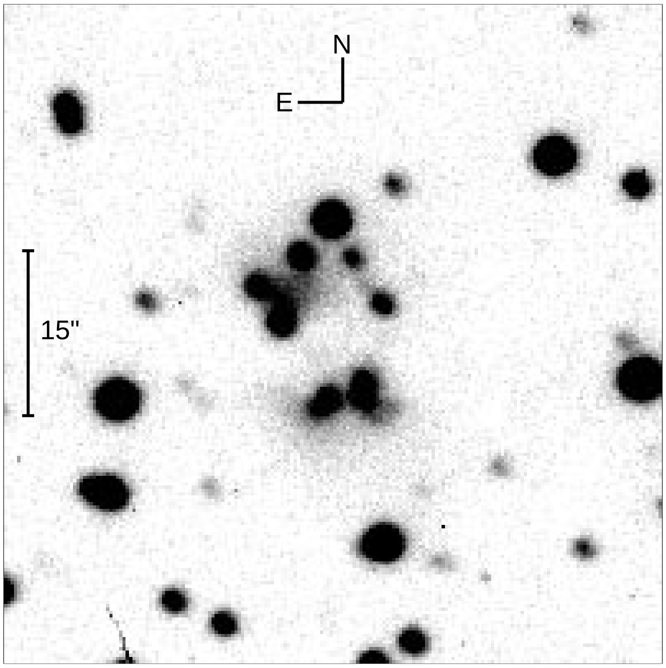

Fig. 4. A CCD $R_{\rm c}$-band frame of IRAS 00412+6638

We believe that these objects do not reside at 7 kpc distance, since at the low galactic latitude of 4° we would expect a high interstellar extinction along such a distance in this longitude region. At 0.4 kpc, the angular extent of about 15″ corresponds to 0.03 pc, a reasonable value for a star forming region, where we see the brightest dozen members in Fig. 4. The moderate extinction (note that we see glimpses of the stars even on the blue-sensitive POSS print) on the one hand, and the presence of CO emission on the other may be interpreted that the bulk of the dense nebular material seems to be located on the far end of the cloud, i.e. we see the stars protruding from the cloud in our direction.

4.2. *Cas 1, a dwarf irregular galaxy*

The nature of this object (number G129.56+07.09 in Table 2) was originally revealed by Weinberger 1995 and proven as a nearby dwarf irregular galaxy by Huchtmeier et al. 1995. Here we present a CCD $I_{\rm c}$-band frame, taken with the 1.8 m telescope of the Asiago Observatory, which for the first time shows the brightest stars of the dwarf galaxy resolved (Fig. 5). With an approximate limiting magnitude of $I_{\rm c} \approx 22^{\rm m}$, an estimated galactic interstellar extinction $A_V = 2^{\rm m} \pm 1^{\rm m}$ (Weinberger 1995), corresponding to $A_I = 1\overset{\rm m}{.}1$, and a distance of 3 Mpc, the stars visible in Cas 1 would have an absolute magnitude of at least $M_I \approx -7^{\rm m}$, i.e. we deal with supergiants. It can be expected that a wealth of further detailed data will be available on this close galaxy within the next few years.

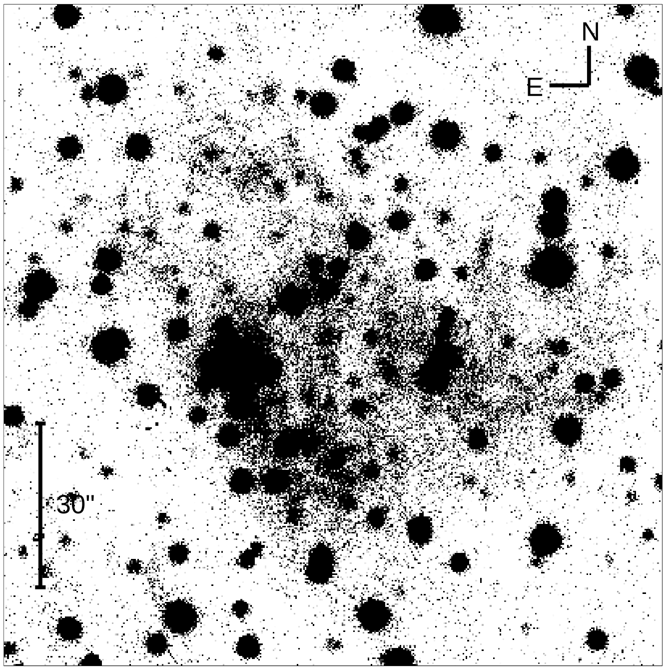

Fig. 5. A CCD I_c-band frame of the close (ca. 3 Mpc) dwarf irregular galaxy Cas 1, resolving the brightest stars

Acknowledgements. This work would not have been possible without the advice and help of several people. One of us (G.L.) is particularly grateful to Drs. W. Saurer and R. Seeberger; in addition, it is a pleasure to thank H. Gratl, Dr. H. Hartl, and last not least the head of the institute, Prof. Dr. J. Pfleiderer, for various support. The allocation of observing time at the Asiago Observatory is gratefully acknowledged. This research was partially supported by the "Fonds zur Förderung der wissenschaftlichen Forschung", project P8325-PHY.

References

Cameron L.M., 1990, A&A 233, 16
Casoli F., Dupraz C., Gerin M., Combes F., Boulanger F., 1986, A&A 169, 281
Hoessel J.G., Elias J.H., Wade R.A., Huchra J.P., 1979, PASP 91, 41
Hubble E., 1934, ApJ 79, 8
Huchtmeier W.K., Lercher G., Seeberger R., Saurer W., Weinberger R., 1995, A&A 293, L33
Kerber F., Lercher G., Saurer W., Seeberger R., Weinberger R., 1994, AG Abstr. Ser. 10, 172
Kraan-Korteweg R.C., 1989, Rev. in Mod. Astr. 2 (Springer), 119
Kraan-Korteweg R.C., Woudt P.A., 1994, Proc. of the 4th DAEC-meeting on: Unveiling large-scale structures behind the Milky Way, p. 89
Kraan-Korteweg R.C., Loan A.J., Burton W.B., et al., 1994, Nat 372, 77
Lercher G., 1994, Proc. of the 4th DAEC-meeting on: Unveiling large-scale structures behind the Milky Way, p. 159
Lynds B.T., 1968, Stars and Stellar Systems VII, 119
McCall M.L., Buta R.J., 1995, AJ 109, 2460
Saito M., Ohtani H., Asomuna A., et al., 1990, PASJ 42, 603
Saito M., Ohtani H., Baba A., et al., 1991, PASJ 43, 449
Seeberger R., Saurer W., Weinberger R., Lercher G., 1994, Proc. of the 4th DAEC-meeting on: Unveiling large-scale structures behind the Milky Way, p. 81
Seeberger R., Saurer, W., Weinberger R., 1995, A&AS (in press)
Wakamatsu K., Hasegawa T., Karoji H., et al., 1994, Proc. of the 4th DAEC-meeting on: Unveiling large-scale structures behind the Milky Way, p. 131
Weinberger R., 1980, A&AS 40, 123
Weinberger R., 1995, PASP 107, 58
Weinberger R., Saurer W., Seeberger R., 1995, A&AS 110, 269
Wheelock S., Gautier T.N., Chillemi J., et al., 1993, IRAS Sky Survey Atlas Explanatory Supplement
Wilking B.A., Mundy L.G., Blackwell J.H., Howe J.E., 1989, ApJ 345, 257
Wouterloot J.G.A., Brand J., 1989, A&AS 80, 149
Yamada T., Takata T., Djamaluddin T., et al., 1993, ApJS 89, 57

Table 2. The catalogue

ZOAG G	α(1950)	δ(1950)	α(2000)	δ(2000)	print	x(mm)	y(mm)	⊘E	⊘E_{bulge}	⊘O	⊘O$_{\mathrm{bulge}}$	t	cross id.
120.00−06.80	0 27 51.2	55 40 51	0 30 37.4	55 57 25	1237	289.9	237.5	0.10 0.10		0.05 0.05			
120.03−07.76:	0 28 38.2	54 43 07	0 31 24.3	54 59 41	1237	286.5	185.8	0.10 0.10		0.10 0.05			
120.03−06.52	0 27 52.4	55 57 21	0 30 38.8	56 13 55	1237	289.0	252.2	0.10 0.10		0.10 0.10			
120.03−05.52	0 27 18.1	56 57 19	0 30 04.7	57 13 53	1237	290.4	305.9	0.10 0.10		0.05 0.05			
120.04−09.37	0 29 29.2	53 07 22	0 32 14.9	53 23 55	1237	283.9	100.2	0.45 0.45	0.15 0.10	0.35 0.35	0.10 0.10		
120.04−09.33	0 29 29.6	53 09 29	0 32 15.4	53 26 02	1237	283.8	102.0	0.15 0.10		0.15 0.10			
120.04+09.33a	0 11 35.1	71 42 44	0 14 20.3	71 59 25	1217	144.2	130.4	0.20 0.15		0.10 0.05			
120.04+09.33b	0 11 37.3	71 42 42	0 14 22.6	71 59 23	1217	144.0	130.3	0.20 0.20		0.15 0.10			
120.06−06.58	0 28 08.4	55 53 47	0 30 54.9	56 10 21	1237	287.1	248.9	0.10 0.10		0.10 0.10			
120.08−09.53	0 29 49.9	52 57 49	0 32 35.7	53 14 22	1237	281.5	91.5	0.15 0.10		0.15 0.10			
120.08−07.65	0 28 52.9	54 50 28	0 31 39.2	55 07 02	1237	284.3	192.3	0.15 0.10		0.15 0.10			
120.08−07.18:	0 28 35.4	55 18 33	0 31 21.8	55 35 07	1237	285.3	217.4	0.20 0.10		0.20 0.05			
120.08−06.38	0 28 08.1	56 06 04	0 30 54.7	56 22 38	1237	286.6	259.9	0.55 0.10	0.05 0.05	0.40 0.10		S	
120.09−09.49	0 29 55.8	53 00 16	0 32 41.7	53 16 49	1237	280.6	93.7	0.55 0.45	0.20 0.15	0.45 0.35	0.10 0.10		a
120.12−09.85:	0 30 18.3	52 38 30	0 33 04.2	52 55 03	1237	278.5	74.1	0.10 0.10		0.05 0.05			
120.12−09.38	0 30 02.6	53 06 40	0 32 48.5	53 23 13	1237	279.5	99.3	0.30 0.10		0.35 0.10			
120.12−09.28	0 29 59.6	53 12 48	0 32 45.6	53 29 21	1237	279.6	104.8	0.40 0.10		0.55 0.10		S?	
120.13−08.51:	0 29 40.4	53 58 51	0 32 26.6	54 15 24	1237	280.3	146.0	0.10 0.10		0.20 0.10			
120.17−09.98	0 30 41.8	52 31 18	0 33 27.7	52 47 51	1237	275.6	67.6	0.15 0.10		0.10 0.10			
120.17+09.44	0 12 59.9	71 50 34	0 15 46.5	72 07 14	1217	138.5	137.6	0.15 0.10		0.10 0.10			
120.18−08.44	0 29 56.9	54 03 26	0 32 43.2	54 19 59	1237	278.0	150.0	0.10 0.10		0.10 0.10			
120.18+08.77	0 14 16.9	71 10 46	0 17 04.1	71 27 26	1217	131.6	102.3	0.15 0.10					
120.19−06.98	0 29 17.5	55 30 53	0 32 04.3	55 47 26	1237	279.5	228.1	0.15 0.10		0.05 0.05			
120.20−08.98	0 30 21.0	53 31 10	0 33 07.3	53 47 43	1237	276.1	121.1	0.15 0.10		0.10 0.05			
120.20−08.06	0 29 54.0	54 26 20	0 32 40.5	54 42 53	1237	277.5	170.4	0.15 0.10		0.05 0.05			
120.25−09.88	0 31 06.5	52 37 44	0 33 52.7	52 54 16	1237	272.0	73.2	0.20 0.10		0.20 0.10			
120.25−09.23	0 30 51.0	53 16 37	0 33 37.3	53 33 09	1237	272.6	107.9	0.40 0.35	0.10 0.10	0.55 0.50	0.10 0.10		
120.25−08.95	0 30 41.6	53 33 07	0 33 28.0	53 49 40	1237	273.3	122.7	0.10 0.10		0.10 0.05			
120.26−04.93:	0 28 38.9	57 34 01	0 31 26.4	57 50 35	1237	278.9	338.1	0.10 0.10					
120.27−09.85	0 31 16.4	52 39 14	0 34 02.6	52 55 46	1237	270.6	74.5	0.10 0.10		0.15 0.10			
120.27−08.63	0 30 40.1	53 52 10	0 33 26.6	54 08 43	1237	272.8	139.7	0.35 0.20	0.10 0.10	0.35 0.20	0.10 0.05		
120.27−07.30	0 30 01.2	55 11 43	0 32 48.1	55 28 16	1237	274.7	210.8	0.15 0.10					
120.27−06.42	0 29 31.5	56 04 39	0 32 18.6	56 21 12	1237	276.3	258.1	0.20 0.10		0.15 0.10			
120.28−09.84	0 31 17.2	52 39 49	0 34 03.4	52 56 21	1237	270.5	75.0	0.10 0.10		0.10 0.05			
120.28−08.65	0 30 46.0	53 51 06	0 33 32.6	54 07 38	1237	272.0	138.7	0.45 0.10		0.50 0.15		S	
120.29−08.04	0 30 29.5	54 27 50	0 33 16.3	54 44 23	1237	272.8	171.5	0.10 0.10		0.15 0.10			
120.30−05.65	0 29 20.7	56 51 06	0 32 08.2	57 07 39	1237	275.7	299.6	0.10 0.10		0.10 0.05			
120.30+09.59	0 14 25.9	72 00 23	0 17 13.9	72 17 03	1217	132.9	146.5	0.20 0.10		0.10 0.05			
120.33−09.19	0 31 20.5	53 18 51	0 34 07.1	53 35 23	1237	268.6	109.8	0.20 0.20	0.10 0.10	0.10 0.10			
120.33−09.17	0 31 21.1	53 20 19	0 34 07.7	53 36 51	1237	268.5	111.1	0.10 0.10		0.15 0.10			
120.33+08.75	0 16 13.3	71 10 46	0 19 02.2	71 27 25	1217	123.3	102.7	0.15 0.15		0.10 0.10			
120.33+09.50	0 14 54.1	71 55 29	0 17 42.5	72 12 09	1217	130.8	142.3	0.15 0.15		0.15 0.10			
120.34−08.07	0 30 53.4	54 26 19	0 33 40.3	54 42 51	1237	269.7	170.0	0.30 0.10		0.30 0.15			
120.36−09.92	0 31 51.6	52 35 45	0 34 38.0	52 52 17	1237	266.0	71.2	0.20 0.10					
120.36−09.33	0 31 37.3	53 10 56	0 34 23.9	53 27 28	1237	266.7	102.6	0.15 0.10		0.10 0.05			
120.36−07.65	0 30 47.3	54 51 10	0 33 34.4	55 07 42	1237	269.6	192.2	0.15 0.10					
120.37−01.91:	0 27 35.3	60 35 08	0 30 24.1	60 51 42	596	317.3	180.1	0.10 0.10		0.10 0.10			
120.39−09.22	0 31 44.1	53 17 40	0 34 30.8	53 34 12	1237	265.5	108.6	0.15 0.10		0.15 0.10			
120.39−07.18	0 30 45.5	55 19 26	0 33 32.8	55 35 58	1237	268.8	217.4	0.10 0.10		0.10 0.05			
120.39−06.85	0 30 36.1	55 39 11	0 33 23.5	55 55 44	1237	269.2	235.1	0.15 0.10		0.10 0.10			
120.39−06.81	0 30 34.0	55 41 45	0 33 21.4	55 58 18	1237	269.4	237.3	0.20 0.10		0.15 0.10			
120.39−06.66	0 30 32.7	55 50 58	0 33 20.2	56 07 31	1237	269.2	245.6	0.20 0.10		0.15 0.10			
120.40+05.65:	0 21 12.9	68 06 24	0 24 03.1	68 23 01	555	89.4	257.2	0.15 0.10		0.10 0.10			
120.41−09.53	0 32 02.5	52 59 06	0 34 49.2	53 15 38	1237	263.7	92.0	0.45 0.15	0.05 0.05	0.45 0.30		S?	
120.42−09.33	0 32 01.8	53 10 54	0 34 48.6	53 27 26	1237	263.4	102.5	0.65 0.45		1.00 0.65		S	b
120.42−08.36	0 31 33.2	54 09 14	0 34 20.2	54 25 46	1237	265.2	154.6	0.20 0.20	0.05 0.05	0.20 0.15			
120.44−08.95	0 31 59.4	53 34 05	0 34 46.3	53 50 37	1237	262.9	123.1	0.30 0.15		0.30 0.15			
120.44−02.45:	0 28 31.0	60 03 07	0 31 19.9	60 19 41	596	313.5	151.2	0.10 0.10		0.05 0.05			
120.45−09.25:	0 32 09.5	53 16 16	0 34 56.3	53 32 48	1237	262.2	107.2	0.10 0.10		0.05 0.05			
120.46−06.76	0 31 03.4	55 45 18	0 33 51.0	56 01 50	1237	265.6	240.4	0.20 0.15		0.15 0.10			
120.47−09.12	0 32 13.4	53 23 38	0 35 00.3	53 40 10	1237	261.4	113.8	0.15 0.10		0.10 0.10			
120.47+08.00	0 19 00.5	70 26 57	0 21 51.1	70 43 35	1217	108.8	64.4	0.35 0.20		0.20 0.20			
120.52−09.65:	0 32 47.9	52 52 12	0 35 34.8	53 08 43	1237	257.8	85.6	0.10 0.10		0.05 0.05			
120.53−07.99	0 32 08.4	54 31 45	0 34 55.9	54 48 17	1237	259.9	174.5	0.10 0.10		0.05 0.05			
120.53−06.04	0 31 11.6	56 28 16	0 33 59.7	56 44 48	1237	263.0	278.6	0.15 0.10					
120.53−04.04	0 30 08.4	58 28 02	0 32 57.1	58 44 35	596	309.0	65.9	0.35 0.15		0.10 0.10			
120.53+09.73:	0 17 04.5	72 10 33	0 19 55.1	72 27 12	1217	122.5	156.1	0.20 0.15		0.15 0.10			
120.54−09.55	0 32 54.1	52 58 40	0 35 41.1	53 15 11	1237	256.8	91.3	0.90 0.15	0.05 0.05	0.85 0.10		S	
120.54+05.61	0 22 41.9	68 05 03	0 25 33.2	68 21 40	555	81.9	256.5	0.45 0.20	0.10 0.05	0.20 0.15			c
120.55−07.11	0 31 53.3	55 24 49	0 34 41.1	55 41 21	1237	260.0	221.8	0.60 0.40	0.10 0.05	0.45 0.20	0.05 0.05	S?	

a) ZWG 557.001 b) UGC 00343 c) IRAS 00227+6805